Indian Journal of Fibre & Textile Research
Vol. 48, September 2023, pp. 268-286
DOI: 10.56042/ijftr.v48i3.6048

Optimisation of mechanical and functional properties of needle-punched nonwoven filter through fibre denier specific carding parameters

Priyal Dixit & S M Ishtiaque[a]

Department of Textile and Fibre Engineering, Indian Institute of Technology Delhi, New Delhi 110 016, India

Received 26 April 2022; revised received and accepted 13 October 2022

An attempt has been made to highlight the significance of the carding parameters (feeder speed, cylinder speed and doffer speed) required for fibre of different deniers for regulating the structure and ultimately the properties of the nonwoven fabric. A three-factor three-level Box-Behnken factorial design has been employed to analyse and optimise the carding parameters. The work focuses on the comprehensive exploration of the functional properties in the light of nonwoven fabric structures. Regression models of nonlinear process are developed to establish the relationship between specific properties of nonwoven fabric and structural indices. The optimised carding parameters specific to fibre denier result in improved filtration performance of the nonwoven fabric having lower values of fabric thickness, mean flow pore size and pressure drop, besides acquiring higher filtration efficiency.

Keywords: Carding, Fibre denier, Functional properties, Mechanical properties, Needle-punched nonwoven, Polyester

1 Introduction

Nonwoven filter fabrics prove to be a versatile class of filter media owing to the wide range of variables they offer to be worked upon to achieve the desired filtration performance. Significant work has been accomplished to explore the role of fibre characteristics[1-3], solid volume fraction and basis length (total fibre length in unit area of nonwoven)[4-6] on mechanical and functional properties of nonwoven fabrics. Attention has been paid by researchers to study the influence of punching parameters of needle-punched nonwoven machines on filtration performances[7-12].

The fibre characteristics and punching variables contribute a significant part in deciding the behaviour of nonwoven fabrics, but the contribution of carding machine variables could not get the due attention of the researchers. Recently, researchers have established that the orientation of fibres in the carded web is significantly influenced by carding machine parameters[13-15]. Roy and Ishtiaque[16,17] have explored the relationship between fibre orientation influenced by carding machine parameters and nonwoven properties. As reported in the literature that a wider range of fibre deniers is being used in filter media, hence the contribution of fibre deniers in deciding the orientation of fibres in carded web is much required to be established. Accordingly, present authors have established that carding parameters play a crucial role in modulating the structure of nonwovens made from fibres of different deniers[18]. Therefore, in the present work, an attempt has been made to optimise fibre-denier-specific carding parameters for improving the physical, mechanical, and functional properties of nonwoven filter fabrics. Further, regression models of nonlinear process are developed to establish the relationship between specific properties of nonwoven fabric and structural indices.

2 Materials and Methods

Polyester fibre of 3, 4 and 6 denier having 64 mm fibre length each were used for the study. Box-Behnken three-variables three-factors design was used to optimize the feeder, cylinder, and doffer speeds of DILO nonwoven machine line having needle punching technique. The actual values of variables corresponding to coded levels are given in Table 1. A three-variable design was repeated for all three considered fibre deniers as per the experimental plan given in Table 2. The basis weight of 300 g/m^2, punch density of 200 punches/cm^2 and needle penetration depth of 10 mm were kept constants for all the samples.

The nonwoven fabrics were tested for basis weight, fabric thickness, fabric bursting strength, mean flow pore size, filtration efficiency and pressure drop.

[a]Corresponding author.
E-mail: S.M.Ishtiaque@textile.iitd.ac.in

2.1 Fabric Characterisation Techniques

The structural indices have been used to determine the properties of the nonwoven fabrics.

Lindsley's technique was used to measure the proportion of curved fibre ends and the coefficient of relative fibre parallelisation in the carded batt[19].

The proportion of curved fibre ends(ρ) was measured by using the following equation:

$$\rho = \left[\frac{E}{E+N}\right] \quad \ldots(1)$$

Thus, more the fibre curliness in carded batt, the more is the value of ρ

The coefficient of relative fibre parallelisation (K_ρ) was measured using the following equation:

$$K_\rho = \left[1 - \frac{E}{(C+E+N)}\right] \times 100 \quad \ldots(2)$$

This parameter (K_ρ) represents the degree of fibre parallelization and straightening in the carded web. Thus, the more the fibre straightening and parallelization in carded web, the more is the value of K_ρ.

where *C* is the weight of combed out portion under the side plate; *E*, the weight of the projected portion from the edge of the front plate after combing; and *N*, the weight of material after combing and cutting under the front plate.

Table 1 — Actual values of variables corresponding to coded levels

Variables	Levels		
	-1	0	1
Feeder speed (A), m/min	0.14	0.19	0.24
Cylinder speed (B), m/min	100	175	250
Doffer speed (C), m/min	4	6	8

2.2 Anisotropy of Inclination Angle of Fibres

Anisotropy of the inclination angle of fibre is important to both structure and properties of nonwoven fabrics because the arrangement of fibres and their orientation plays a crucial role in determining the properties of nonwoven fabrics. The histogram of fibre inclination was devised with the help of a mathematical model[20]as given below:

$$p(\psi) = \frac{1}{\pi}\frac{\eta}{\eta^2-(\eta^2-1)cos^2(\psi)} \quad \ldots(3)$$

where ψ is the probability density function of all inclination angle ψ; and η, the measure of anisotropy of fibre orientation in fibre web.

2.3 Basis Weight

Basis weight was measured following the ASTM standard D6242. Ten specimens, each measuring 10.2 cm × 10.2 cm, were randomly taken from samples and weighed on electronic balance.

2.4 Fabric Thickness

ASTM D1777-96 standard was used to measure the fabric thickness using Essdiel thickness gauge at a pressure of 20gf/cm². Ten readings were taken for the measurement of fabric thickness and the average was calculated.

2.5 Mean Flow Pore Size

The capillary flow porometer was used to measure the mean flow pore size of the fabrics. The fabrics were wetted with a low surface tension liquid and placed in a sealed chamber that was then pressurized with nitrogen gas. Ten readings were taken for each sample and the average was calculated.

Table 2 — Properties of fabrics made from fibres of different deniers at different carding parameters

Carding parameters			Fabric thickness mm			Bursting strength bar			Mean flow pore size, µm			Filtration efficiency %			Pressure drop Pa		
Feeder speed m/min	Cylinder speed m/min	Doffer speed m/min	3 den	4 den	6 den	3 den	4 den	6 den	3 den	4 den	6 den	3 den	4 den	6 den	3 den	4 den	6 den
0.24	175	8	2.49	2.84	3.84	17.68	14.98	13.41	26.04	30.99	42.56	84.83	73.80	57.62	100.19	89.57	71.14
0.24	175	4	2.86	3.11	4.31	18.32	15.74	13.73	28.31	31.13	44.59	71.36	59.23	51.78	85.80	73.59	59.74
0.14	250	6	2.06	2.31	3.20	16.11	13.87	11.94	21.12	25.56	35.03	94.29	77.31	65.37	107.99	98.29	81.63
0.19	250	8	2.01	2.21	3.13	17.00	14.22	11.86	22.85	26.96	37.65	89.87	75.49	66.52	108.03	92.39	78.03
0.19	175	6	2.48	2.83	3.82	16.53	13.47	12.49	21.28	25.32	35.47	92.63	80.58	56.48	109.14	97.81	80.11
0.14	175	8	2.12	2.31	3.20	17.53	13.64	11.76	21.15	24.74	35.24	86.71	71.97	62.86	105.78	89.42	7418
0.19	100	4	3.07	3.43	4.75	18.85	15.59	13.65	27.50	33.27	44.81	69.83	57.26	54.98	83.02	72.79	60.34
0.24	100	6	3.06	3.36	4.77	18.12	15.87	13.79	28.39	33.50	45.93	71.66	60.20	49.15	84.76	73.68	62.03
0.24	250	6	2.26	2.57	3.48	17.56	15.06	13.23	26.02	30.96	42.41	85.23	75.15	57.49	101.75	89.99	73.68
0.14	100	6	2.63	2.87	3.98	18.04	15.35	13.47	23.50	27.49	38.80	74.91	62.18	55.68	92.84	77.26	63.86
0.19	250	4	2.38	2.67	3.69	17.88	14.85	12.86	25.12	30.40	41.18	82.80	67.90	60.26	96.31	86.32	69.02
0.19	175	6	2.53	2.78	3.95	16.59	13.42	12.46	21.28	25.11	35.26	92.35	77.57	60.85	108.03	94.94	81.11
0.19	175	6	2.48	2.83	3.82	16.56	13.52	12.51	21.28	25.32	35.26	92.63	80.58	59.14	108.17	97.81	80.64
0.19	100	8	2.59	2.82	3.91	18.56	15.43	13.47	25.22	29.51	41.22	70.45	58.47	56.86	86.29	72.65	61.26
0.14	175	4	2.66	2.98	4.12	17.28	14.63	12.65	23.42	28.34	38.68	87.16	71.47	62.03	100.83	90.87	76.82

2.6 Fabric Bursting Strength

The ASTM D3786 standard was used to measure the bursting strength of the fabric using a digital bursting strength tester. Ten randomly selected specimens were tested for each sample.

2.7 Filtration Efficiency and Pressure Drop

A purpose-built air filtration setup as shown in Fig. 1 was used to evaluate the filtration efficiency and pressure drop of the nonwoven fabrics[3]. Overall, ten tests were conducted for the measurement of filtration efficiency and pressure drop, and the average was calculated.

The filtration efficiency is related to the upstream particle count (U_p) and downstream particle count (D_p). Accordingly, filtration efficiency is calculated using the following equation:

$$\text{Filtration efficiency, \%} = \frac{U_p - D_p}{U_p} \times 100 \quad \ldots(4)$$

where U_p is the upstream particle count; and D_p, the down stream particle count.

3 Results and Discussion

3.1 Fabric Thickness

The results of the thickness of fabrics made from the fibre of different deniers influenced by carding parameters are shown in Table 2.

Table 3 summarises the effect of carding parameters on various structural indices for nonwoven fabrics made from fibre of different deniers.

The variance analysis was carried out for nonwoven fabrics made from the fibre of different deniers. However, to avoid repetition, variance analysis of only 3 denier fibre is reported and results are shown in Table 4.

The response surface equations for fabric thickness, in terms of coded factors and significant model terms, are represented in the following equations, having R^2 values of 0.935, 0.928 and 0.952 for 3, 4 and 6 denier fibres respectively:

3 denier fabric

$$\text{Thickness} = 2.5120 + 0.1483 \times A - 0.3293 \times B - 0.2192 \times C - 0.0574 \times AB + 0.0438 \times AC + 0.0263 \times BC \quad \ldots(5)$$

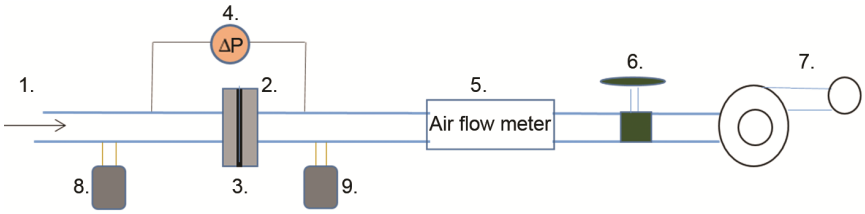

Fig. 1 — Schematics of air filter test rig [1-Air inlet, 2- Rubber coated sample holder, 3-Test filter media, 4-Digital pressure gauge, 5-Air flow meter, 6-Flow control valve, 7-Suction pump, 8-Upstream particle counter and 9-Downstream particle counter]

Table 3 — Structural indices of nonwoven fabrics made of fibres of different deniers at different carding parameters

Carding parameters			3 Den			4 Den			6 Den		
Feeder speedm/min	Cylinder speed m/min	Doffer speed m/min	Proportion of curved fibre ends	Coefficient of relative fibre parallelisation	Anisotropy of inclination angle of fibre	Proportion of curved fibre ends	Coefficient of relative fibre parallelisation	Anisotropy of inclination angle of fibre	Proportion of curved fibre ends	Coefficient of relative fibre parallelisation	Anisotropy of inclination angle of fibre
0.24	175	8	0.2850	0.5251	2.67	0.2570	0.5635	3.12	0.2122	0.5977	3.25
0.24	175	4	0.3875	0.4417	2.34	0.3526	0.4523	2.64	0.2897	0.542	2.8
0.14	250	6	0.2337	0.5836	3.15	0.2238	0.5903	3.35	0.1744	0.6683	3.58
0.19	250	8	0.2470	0.5563	2.83	0.2247	0.5764	3.42	0.1826	0.6612	3.6
0.19	175	6	0.2448	0.5733	2.93	0.2127	0.6153	3.33	0.2317	0.5919	3.53
0.14	175	8	0.2824	0.5367	2.71	0.2594	0.5495	3.38	0.1739	0.6692	3.62
0.19	100	4	0.3952	0.4322	2.19	0.3532	0.4472	2.68	0.2891	0.545	2.97
0.24	100	6	0.3718	0.4436	2.37	0.3384	0.4596	2.56	0.2949	0.4973	2.71
0.24	250	6	0.2844	0.5275	2.69	0.2560	0.5662	3.04	0.2127	0.5968	3.25
0.14	100	6	0.3524	0.4637	2.45	0.3207	0.4748	2.85	0.2629	0.5754	3.14
0.19	250	4	0.3105	0.5125	2.60	0.2825	0.5284	3.14	0.2099	0.6107	3.32
0.19	175	6	0.2459	0.5716	2.85	0.2227	0.5923	3.25	0.1843	0.6114	3.42
0.19	175	6	0.2380	0.5734	2.89	0.2166	0.6153	3.16	0.2107	0.6085	3.39
0.19	100	8	0.3882	0.4361	2.26	0.3596	0.4465	2.75	0.2774	0.5696	3.1
0.14	175	4	0.2813	0.5395	2.79	0.2588	0.5557	3.18	0.1835	0.6244	3.4

Table 4 — Variance analysis of thickness of nonwoven fabrics made from3 denier fibres

Source	Sum of squares	df	Mean square	F-value	p-value	Significance
Model	1.45	6	0.2420	323.51	< 0.0001	Significant
A-Feeder speed	0.1759	1	0.1759	235.25	< 0.0001	
B-Cylinder speed	0.8676	1	0.8676	1160.04	< 0.0001	
C-Doffer speed	0.3846	1	0.3846	514.21	< 0.0001	
AB	0.0132	1	0.0132	17.59	0.0030	
AC	0.0077	1	0.0077	10.28	0.0125	
Residual	0.0060	8	0.0007			
Lack of fit	0.0044	6	0.0007	0.9070	0.6090	Not significant
Pure error	0.0016	2	0.0008			
Cor total	1.46	14				

4 denier fabric

$$\text{Thickness} = 2.7959 + 0.1774 \times A - 0.3410 \times B - 0.2513 \times C - 0.0574 \times AB + 0.0989 \times AC + 0.0388 \times BC \quad ...(6)$$

6 denier fabric

$$\text{Thickness} = 3.8650 + 0.2372 \times A - 0.4884 \times B - 0.3497 \times C - 0.1285 \times AB + 0.1115 \times AC + 0.0717 \times BC \quad ...(7)$$

These equations are used to draw the 3D surface plots of carding parameters in relation to the thickness of the fabric.

Figures 2 (a) - (c) show the 3D surface plots of cylinder speed *vs* doffer speed, at constant feeder speed in relation to fabric thickness made from considered fibre deniers. The results of 3D surface plots and Eqs (5) - (7) show a reduction in fabric thickness with the increase in cylinder and doffer speeds at a constant feeder speed of 0.19 m/min. The obtained trends are found to be applicable to all the considered fibre deniers. The increase in centrifugal force on fibres due to increased cylinder speed, which, in turn, is responsible for increased fibre transfer efficiency with a subsequent decrease in cylinder loading leads to better fibre opening and more fibre individualization. This results in fibre straightening and parallelization, there by reducing the fibre inclination angle and increasing the fibre extent in the carded web.

However, an increase in doffer speed reduces trailing hooks with an increase in the leading as well as both ends' hooks. The increase in doffer as well as cylinder speeds provides positive results in terms of hooks in the carded web which increases fibre extent. An initial increase and then a slight decrease in the values of the coefficient of relative fibre parallelization and anisotropy of inclination angle of the fibre, but a decrease followed by a slight increase in the proportion of curved fibre ends with the increase of cylinder and doffer speeds is known. The measured structural indices are positively influenced by fibre straightening and parallelization in the carded web. Hence, the fibres are more adequately packed, which causes reduction in fabric thickness. The increase in both cylinder and doffer speeds at different feeder speeds depicts a significant decrease in fabric thickness but a small increase in fabric thickness with the increase in feeder speed. Similar trends are also observed for all fibre deniers. However, increased feeder speed increases the thickness of the feed material which results in lesser penetration of wire points in the feed material. Hence, licker-in provides fewer points per fibre, which reduces the opening of fibre tufts. Whereas, increased feeder speed decreases the cylinder-to-doffer transfer of fibres, thereby increasing the loading of fibres on the cylinder. Accordingly, an increased feeder speed confirms the reduction in the values of coefficient of relative fibre parallelization and anisotropy of the inclination angle of fibre, but an increase in the value of the proportion of curved fibre ends. However, a progressive increase in feeder, cylinder and doffer speeds leads to a reduction in fabric thickness. Therefore, it can be concluded that the influence of the feeder speed on the fabric thickness is taken care of by the considered cylinder and doffer speeds. Further, Table 2 depicts an increase in fabric thickness with increased fibre denier. The fibre diameter becomes the key factor in deciding the fabric thickness. Smaller diameter fibre reduces fibre-fibre spacing, leading to more adequately packed fibres within the fabric, resulting in lesser fabric thickness. Additionally, an increase in fibre denier enhances its flexural rigidity, resulting in increased resistance towards bending and consequentially increased fabric thickness.

Figures 2 (d) - (f) show the 3D surface plots of feeder speed *vs* doffer speed, at a constant cylinder speed of 175 m/min in relation to fabric thickness made from considered deniers of fibre. An increase in fabric thickness is noticed with increased feeder speed at a constant cylinder speed due to fibre disorientation

in the carded web. However, increased doffer speed depicts a decrease in fabric thickness at different cylinder speeds which is due to better fibre orientation in the carded web. A small reduction in fabric thickness is noticed with an increase in both feeder and doffer speeds at respective cylinder speeds. However, an increase in cylinder speed shows moderate reduction in fabric thickness. The slight reduction in fabric thickness is mainly due to the dominance of increased doffer speed over feeder

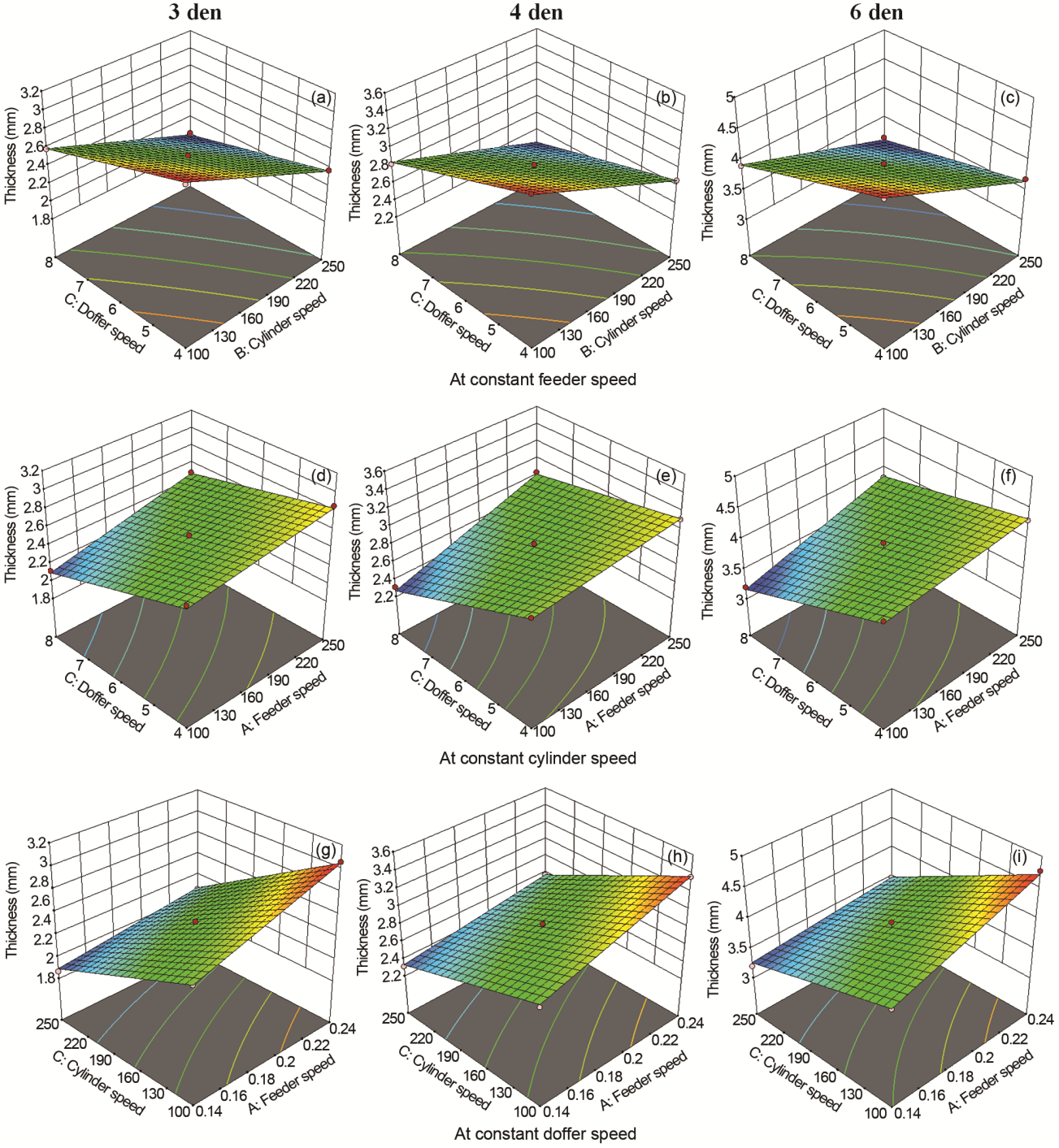

Fig. 2 — Thickness of nonwoven fabric made of fibre of different deniers: (a) - (c) — doffer speed *vs* cylinder speed at constant feeder speed of 0.19 m/min; (d) - (f)— doffer speed *vs* feeder speed at constant cylinder speed of 175 m/min; and (g) - (i)— cylinder speed *vs* feeder speed at constant doffer speed of 6 m/min

speed, causing improved fibre straightening and parallelisation, thus resulting in enhanced fibre orientation in the carded web. The combined effect of the increase in feeder, cylinder and doffer speed results in a reduction in fabric thickness. Here again, the influence of feeder speed to increase the fabric thickness is overruled by the increase of cylinder and doffer speeds, which results in overall reduction in fabric thickness. It is interesting to note that the observed trends were equally applicable to all considered fibre deniers. It is observed that increase in fibre denier increases the thickness of the fabrics. Therefore, it is concluded that the obtained trends of fabric thickness, influenced by carding parameters, are regulated by coefficient of relative fibre parallelization, anisotropy of the inclination angle of fibre and proportion of curved fibre ends. The justifications given above are equally valid for the obtained trends.

Figures 2 (g) - (i) show the 3D surface plots of cylinder speed *vs* feeder speed, at a constant doffer speed of 6 m/min in relation to fabric thickness made from considered deniers of fibre. The results indicate a small increase in fabric thickness with increased feeder speed followed by a significant reduction with increased cylinder speed at a constant doffer speed. An increase in both feeder and cylinder speeds at different doffer speeds depict a moderate reduction in fabric thickness, while an increased doffer speed results in moderate reduction in fabric thickness. The dominance of cylinder and doffer speeds inherently retains their respective roles in controlling the fabric thickness. The fabric thickness value shows a significant decrease with increased feeder, cylinder and doffer speeds for all considered fibre deniers. Therefore, it can be concluded that cylinder speed plays a more prominent role in improving the fibre orientation in the carded web followed by doffer speed, but the influence of feeder speed does not get reflected in the overall orientation of the carded web. Therefore, improved fibre orientation in the carded web, measured by coefficient of relative fibre parallelization, anisotropy of inclination angle of fibre and the proportion of curved fibre ends, influenced by machine parameters, is responsible for the reduction in fabric thickness. However, it is observed that an increase in fibre denier depicts an increase in the thickness of the nonwoven fabric. The increase in fabric thickness influenced by fibre denier is justified, as stated above.

3.1.1 Optimisation of Carding Parameters in Relation to Fabric Thickness

The carding parameters are optimised for nonwoven fabrics made from fibres of different deniers, keeping fabric thickness to a minimum. It is observed that the feeder speed, cylinder speed and doffer speed for nonwoven fabrics made of 3 denier fibre are 0.14 m/min, 225.51 m/min and 7.12 m/min respectively. Similarly, the optimised feeder, cylinder, and doffer speeds for the minimum value of fabric thickness made up of 4 denier fibres are0.14 m/min, 132.71 m/min and 4.65 m/min respectively and for 6 denier fibre, the feeder, cylinder, and doffer speeds are found to be 0.15 m/min, 100.56 m/min and 4.04 m/min respectively. These results reveal the corresponding minimum thickness of fabrics made of fibres of different deniers at various combinations of carding parameters. Moreover, cylinder and doffer play a significant role in governing the fabric thickness, owing to the straightening and parallelisation they impart to the fibres, which results in better consolidation of fibre and thus lower fabric thickness.

3.1.2 Influence of Structural Indices on Fabric Thickness

The above discussion signifies the importance of structural indices to modulate the fabric thickness. A regression model of the nonlinear process is established among the thickness of nonwoven fabric and proportion of curved fibre ends, coefficient of relative fibre parallelization and anisotropy of inclination angle of fibres, separately as shown in the following equations.

3 denier fabric

$$\text{Thickness} = 16.5796 + 78.5362 \times X_1 - 26.8830 \times X_2 + 29.0275 \times X_3 - 111.6870 \times X_1^2 + 262.0040 \times X_2^2 - 5.1485 \times X_3^2 \quad \ldots(8)$$

4 denier fabric

$$\text{Thickness} = 9.1862 + 55.7711 \times X_1 - 23.7127 \times X_2 - 7.1575 \times X_3 - 79.1442 \times X_1^2 + 35.0029 \times X_2^2 + 0.9440 \times X_3^2 \quad \ldots(9)$$

6 denier fabric

$$\text{Thickness} = 20.6869 - 101.9230 \times X_1 + 69.8095 \times X_2 + 13.3846 \times X_3 + 202.9390 \times X_1^2 + 38.4565 \times X_2^2 - 1.8907 \times X_3^2 \quad \ldots(10)$$

where X_1 is the proportion of curved fibre ends; X_2, the coefficient of relative fibre parallelisation and X_3, the anisotropy of inclination angle of fibre.

The obtained R^2 values of the above equations are 0.767, 0.804 and 0.837 respectively, indicating that the structural indices play a crucial role in determining fabric thickness. The influence of

proportion of curved fibre ends on fabric thickness is found to be maximum followed by the coefficient of relative parallelisation and anisotropy of inclination angle of fibre. Reduction in the proportion of curved fibre ends is accompanied by a decrease in the number of hooks and loops in the fibres, resulting in more fibre straightening. This further leads to an increase in the coefficient of relative fibre parallelisation. Accordingly, fibres get better oriented, as also confirmed by the increase in anisotropy values. Fibre straightening and parallelization create closed packed structure, which ultimately leads to reduction in fabric thickness.

3.2 Bursting Strength

Table 2 summarises the effect of carding parameters on bursting strength of nonwoven fabrics. The variance analysis of bursting strength of fabrics made of 3, 4 and 6 denier fibres is carried out. Table 5 shows the variance analysis of only 3 denier fibre.

The response surface equations for bursting strength of fabrics in terms of coded factors and significant model terms are represented in the following equations having R^2 values of 0.953, 0.895 and 0.938 respectively:

3 denier fabric

$$\text{Bursting strength} = 19.1738 + 1.0055 \times A - 1.7704 \times B - 0.5973 \times C + 0.8793 \times AB - 0.4966 \times AC - 0.6920 \times BC + 1.7024 \times A^2 + 1.8452 \times B^2 + 2.49284 \times C^2 \quad ...(11)$$

4 denier fabric

$$\text{Bursting strength} = 13.4700 + 0.5200 \times A - 0.5300 \times B - 0.3175 \times C + 0.1675 \times AB + 0.0575 \times AC - 0.1175 \times BC + 0.6462 \times A^2 + 0.9212 \times B^2 + 0.6312 \times C^2 \quad ...(12)$$

Table 5 — Variance analysis of bursting strength of fabrics made of 3 denier fibre

Source	Sum of squares	df	Mean square	F-value	p-value	Significance
Model	82.35	9	9.15	33.91	0.0006	Significant
A-Feeder speed	8.09	1	8.09	29.97	0.0028	
B-Cylinder speed	25.07	1	25.07	92.91	0.0002	
C-Doffer speed	2.85	1	2.85	10.58	0.0226	
AB	3.09	1	3.09	11.46	0.0196	
BC	1.92	1	1.92	7.10	0.0447	
A^2	10.70	1	10.70	39.65	0.0015	
B^2	12.57	1	12.57	46.58	0.0010	
C^2	22.94	1	22.94	85.03	0.0003	
Residual	1.35	5	0.2699			
Lack of fit	1.30	3	0.4331	17.28	0.0552	Not significant
Pure error	0.0501	2	0.0251			
Cor total	83.70	14				

6 denier fabric

$$\text{Bursting strength} = 12.4867 + 0.5425 \times A - 0.5612 \times B - 0.2987 \times C + 0.2425 \times AB + 0.1425 \times AC - 0.2050 \times BC + 0.2742 \times A^2 + 0.3467 \times B^2 + 0.1267 \times C^2 \quad ...(13)$$

They were used to draw the 3D surface plots of considered carding parameters in relation to bursting strength of nonwoven fabric.

Figures 3 (a) - (c) show the 3D surface plots of cylinder speed *vs* doffer speed at different feeder speeds in relation to the bursting strength of nonwoven fabric made from 3 denier, 4 denier, and 6 denier fibres respectively. The above equations along with their corresponding 3D surface plots reveal an initial decrease and then an increase in bursting strength of fabric made of 3 denier fibres with the increase in cylinder speed. The same trends are also observed for other fibre deniers. It is known that bursting strength is determined by applying multidirectional load on the fabric. Both extensibility of fibres and fibre orientation play a crucial role in determining the bursting strength of a fabric. As discussed previously, the increase in cylinder speed imparts more straightening and parallelisation to the fibres, and hence, fibres get better oriented. This is also confirmed by the reduction in values of the proportion of curved fibre ends and increase in coefficient of relative fibre parallelisation accompanied by higher anisotropy of inclination angle of fibre values. These structural characteristics are responsible for a reduction in bursting strength of the fabric. Further increase in cylinder speed disorients the fibres, as also revealed by the higher value of proportion of curved fibre ends, lower coefficient of relative fibre parallelisation and reduced anisotropy of inclination angle of fibre. This increases the bursting strength of the fabrics. The bursting strength follows a decrease and then increase with the increase in doffer speed. This trend is due to the changes in fibre orientation with the increase in doffer speed. The increase in both cylinder and doffer speeds at constant feeder speed leads to an initial decrease and then an increase in bursting strength. The results of bursting strength very well correspond with the trends in measured structural indices, as discussed above. The increase in the speeds of the feeder, cylinder and doffer follows an increase and then decrease in bursting strength. It is also observed that bursting strength decreases as fibre denier increases, because coarser fibres have higher bending rigidity and hence rupture easily as compared to finer fibres, which impart lower bursting strength.

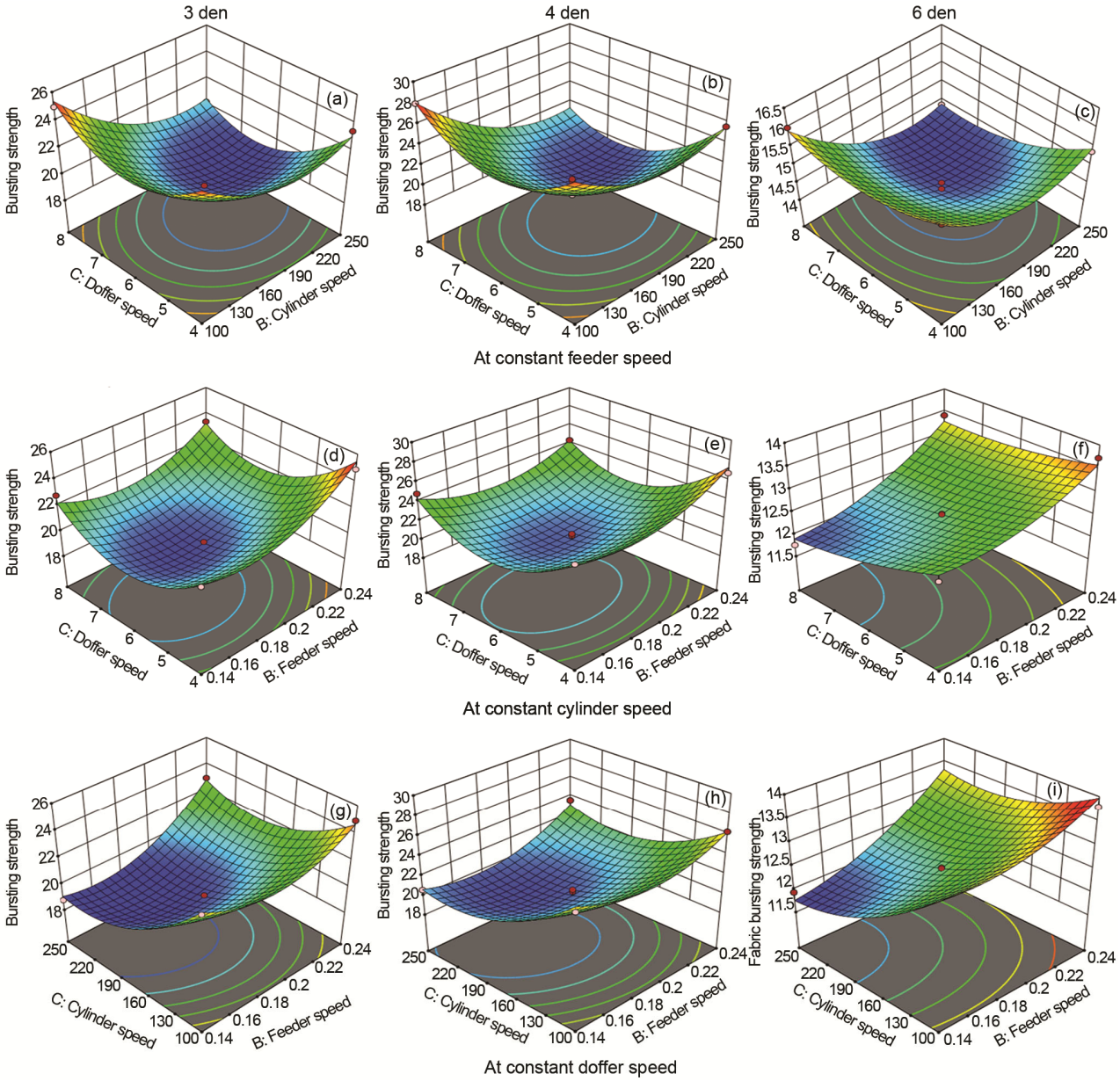

Fig. 3 — Bursting strength of nonwoven fabric made of fibre of different deniers: (a) - (c) — doffer speed *vs* cylinder speed at constant feeder speed of 0.19 m/min; (d)-(f) — doffer speed *vs* feeder speed at constant cylinder speed of 175 m/min, and (g) - (i) — cylinder speed *vs* feeder speed at constant doffer speed of 6 m/min

Figures 3 (d) - (f) show the 3D surface plots of feeder speed *vs* doffer speed at different cylinder speeds in relation to the bursting strength of nonwoven fabric made from 3 denier, 4 denier and 6 denier fibres respectively.

The bursting strength of the fabric shows a slight initial decrease and then an increase with increase in feeder speed. Similarly, an increase in doffer speed leads to a decrease and then an increase in bursting strength. It is found that the bursting strength decreases and then increases with an increase in both feeder and doffer speeds. The changes in fibre orientation in the fabric induced by the increase in feeder and doffer speeds, as revealed by the measured structural indices, influence the bursting strength. The bursting strength decreases with an increase in fibre denier due to reasons discussed earlier.

Figures 3 (g) - (i) show the 3D surface plots of feeder speed *vs* cylinder speed at different doffer speeds in relation to bursting strength of nonwoven fabrics made from 3, 4 and 6 denier fibres respectively. Bursting strength shows a decrease

followed by an increase with the increase in cylinder and feeder speeds at a constant doffer speed of 6 m/min. The bursting strength further shows similar trends during the simultaneous increase in feeder, cylinder and doffer speeds. The increase in centrifugal force on fibres due to the increase in cylinder speed leads to better fibre opening and more fibre individualization which subsequently results in fibre straightening and parallelization. However, at higher cylinderspeed, the application of high forces on fibre disturbs the fibre orientation on the other hand lesser penetration of wire point in the feed material due to high feed rate reduces the opening of fibre tufts, which increases the loading of fibres on the cylinder. It is further observed that bursting strength of the fabric increases as fibre denier decreases, due to the reasons explained above.

3.2.1 Optimisation of Carding Parameters in Relation to Fabric Bursting Strength

The carding parameters have been optimised for nonwoven fabrics made from fibres of different deniers by targeting the moderate value of bursting strength of the fabrics. The moderate bursting strength of fabric made of 3 denier fibres is achieved at 0.14 m/min, 158.9 m/min and 5.66 m/min of feeder, cylinder, and doffer speeds respectively. Similarly, the moderate bursting strength of fabrics made of 4 denier fibres is recorded at0.14 m/min, 166.72 m/min and 6.21 m/min of feeder, cylinder, and doffer speeds respectively. But for nonwoven fabrics made of 6 denier fibres, the feeder, cylinder, and doffer speeds are 0.14 m/min, 189.72 m/min and 4.78 m/min respectively. It is also observed that the corresponding moderate value of bursting strength leads to different combinations of carding parameters for fibres of different deniers. It can be noticed further that cylinder and doffer speeds play a crucial role in determining the bursting strength.

3.2.2 Influence of Structural Indices on Fabric Bursting Strength

A regression model of nonlinear process has been established between bursting strength of the fabrics made of fibres of different deniers and proportion of curved fibre ends, coefficient of relative fibre parallelization and anisotropy of inclination angle of fibres as shown in the following equations having R^2 values as 0.932, 0.923 and 0.948 respectively:

3 denier fabric

$$\text{Bursting strength} = -4.8432 - 26.7398 \times X_1 + 208.6640 \times X_2 - 17.3763 \times X_3 + 45.5327 \times X_1^2 - 204.9630 \times X_2^2 + 2.7715 \times X_3^2 \quad ...(14)$$

4 denier fabric

$$\text{Bursting strength} = -35.9252 - 25.9222 \times X_1 + 287.2210 \times X_2 - 20.0523 \times X_3 + 107.6570 \times X_1^2 - 248.6380 \times X_2^2 + 3.0742 \times X_3^2 \quad ...(15)$$

6 denier fabric

$$\text{Bursting strength} = 17.0066 + 39.3409 \times X_1 - 153.0080 \times X_2 + 27.1378 \times X_3 - 95.0465 \times X_1^2 + 127.8320 \times X_2^2 - 4.7555 \times X_3^2 \quad ...(16)$$

The obtained R^2 values indicate a strong correlation between bursting strength of fabrics made of fibres of different deniers and structural indices. Bursting strength is influenced more likely by coefficient of relative fibre parallelisation followed by the proportion of curved fibre ends and anisotropy of inclination angle of the fibre. Increase in coefficient of relative fibre parallelisation and anisotropy of inclination angle of fibre along with the reduction in the proportion of curved fibre ends result in more straighter and parallel fibres. Since the bursting force is multidirectional, the better-oriented fibres lead to lower bursting strength. On the contrary, a reduction in coefficient of relative fibre parallelisation along with anisotropy of inclination angle of fibre and increase in proportion of curved fibre ends increase the bursting strength.

3.3 Mean Flow Pore Size

The results of mean flow pore size of fabrics made of fibres of different deniers influenced by carding parameters are shown in Table 2. Table 6 provides the results of variance analysis of mean flow pore size of nonwoven fabrics made of 3 denier fibres.

Table 6 — Variance analysis of mean flow pore size of 3 denier nonwoven fabric

Source	Sum of squares	df	Mean square	F-value	p-value	Significance
Model	88.86	9	9.87	31.43	0.0007	Significant
A-Feeder speed	34.32	1	34.32	109.25	0.0001	
B-Cylinder speed	11.50	1	11.50	36.59	0.0018	
C-Doffer speed	5.41	1	5.41	17.23	0.0089	
AB	5.18	1	5.18	16.48	0.0097	
AC	3.42	1	3.42	10.89	0.0215	
A^2	7.48	1	7.48	23.80	0.0046	
B^2	9.55	1	9.55	30.39	0.0027	
C^2	16.21	1	16.21	51.61	0.0008	
Residual	1.57	5	0.3141			
Lack of fit	0.4809	3	0.1603	0.2941	0.8306	Not significant
Pure error	1.09	2	0.5449			
Cor total	90.43	14				

The response surface equations for mean flow pore size of fabrics made of 3, 4 and 6 deniers of fibre in terms of coded factors and significant model terms are represented in the following equations having R^2 values of 0.914, 0.882 and 0.896 respectively:

3 denier fabric

$$\text{Mean flow pore size} = 22.7367 + 2.0712 \times A - 1.1987 \times B - 0.8225 \times C + 1.1375 \times AB + 0.9250 \times AC + 0.0950 \times BC + 1.4229 \times A^2 + 1.6079 \times B^2 + 2.0954 \times C^2 \quad \ldots (17)$$

4 denier fabric

$$\text{Mean flow pore size} = 25.2523 + 2.5561 \times A - 1.2372 \times B - 1.3666 \times C - 0.1521 \times AB + 0.8644 \times AC + 0.0809 \times BC + 1.4450 \times A^2 + 2.6815 \times B^2 + 2.1008 \times C^2 \quad \ldots (18)$$

6 denier fabric

$$\text{Mean flow pore size} = 35.3323 + 3.4673 \times A - 1.8105 \times B - 1.5744 \times C + 0.0635 \times AB + 0.3520 \times AC + 0.0165 \times BC + 2.1312 \times A^2 + 3.0773 \times B^2 + 2.8058 \times C^2 \quad \ldots (19)$$

3D surface plots of considered carding parameters in relation to mean flow pore size of the fabric are drawn with the help of these equations.

Figures 4 (a) - (c) show the 3D surface plots of cylinder speed *vs* doffer speed at a constant feeder speed in relation to mean flow pore size of fabrics made from fibres of different deniers. From the above-mentioned equations and corresponding 3D surface plots, it is inferred that the mean flow pore size of nonwoven fabrics made from 3 denier fibres shows an initial decrease and then increases with an increase in cylinder and doffer speeds. Similar trends are also registered by the fabrics made from other denier fibres.

The observed trends are highly influenced by measured structural indices. The increase in cylinder and doffer speeds at constant feeder speed, as established earlier, results in a reduction in proportion of curved fibre ends, besides increasing the coefficient of relative fibre parallelisation and enhancing anisotropy of inclination angle of fibre and tortuosity factor. These factors are responsible for better orientation of fibres and provide a more packed structure, leading to a reduction in mean flow pore size of the nonwoven fabrics. However, further increase in cylinder and doffer speeds at a constant feeder speed invites disorientation of the fibres, which leads to an increase in mean flow pore size. It is to be noted that fabric thickness also plays a crucial role in determining the mean flow pore size. Fabrics with lesser thickness possess smaller mean flow pore size. The simultaneous increase in feeder, cylinder and doffer speeds provides an initial increase and then a decrease in mean flow pore size. Fabrics made of fibres of other deniers also follow the identical trend, as observed in case of 3 denier fibre. It is further observed that the mean flow pore size records an increase with the increase in fibre denier. The mean flow pore size of the fabric is governed by the diameter of respective fibre and orientation of fibre in carded web is influenced by carding parameters. It is obvious that the smaller diameter fibre will provide a greater number of smaller mean flow pore size in the fabric as compared to larger diameter fibre. Moreover, the proportion of curved fibre ends shows an increase, and coefficient of relative fibre parallelisation and anisotropy of inclination angle of fibre show a decrease with the decrease in fibre denier. Therefore, fibre diameter as well as fibre orientation of corresponding fibre in carded web decide the mean flow pore size.

Figures 4 (d) - (f) show the 3D surface plots of feeder speed *vs* doffer speed, at a constant cylinder speed in relation to mean flow pore size of fabrics made from fibre of different deniers. The mean flow pore size of fabrics made from 3 denier fibre shows a decrease and then an increase with the increase in feeder and doffer speeds at constant cylinder speed. The mean flow pore size of fabrics made from other denier fibres also follow identical trends, as observed in case of 3 denier fibre. With the initial increase in feeder speed, the disorientation of fibres caused by feeder speed is taken care of by cylinder and doffer speeds, which results in a reduction in mean flow pore size. Further increase in feeder speed increases the proportion of curved fibre ends, but reduces coefficient of relative fibre parallelisation and anisotropy of inclination angle of the fibre, which ultimately increases the mean flow pore size. The mean flow pore size shows a decrease and then a slight increase with the increase in doffer speed. The initial decrease in mean flow pore size is due to the improvement in fibre orientation, but a later decrease is influenced by the disorientation of fibre while increasing the doffer speed. The increase in both feeder and doffer speeds at a respective cylinder speed shows a decrease and then an increase in the mean flow pore size. Increase in cylinder speeds also follows a decreasing and increasing trend of mean flow pore size. The simultaneous increase in feeder, cylinder and doffer speeds also leads to an initial

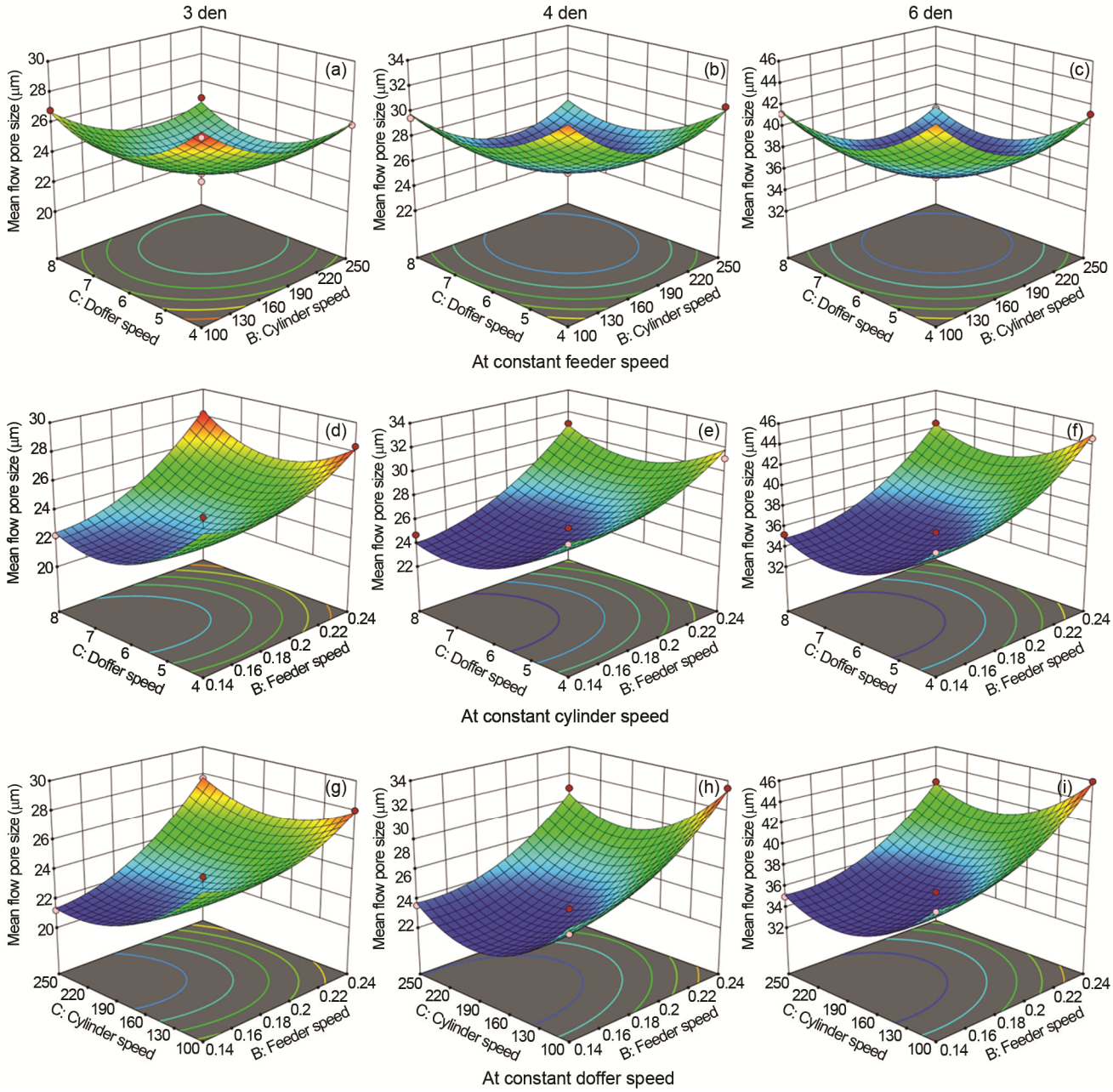

Fig. 4 — Mean flow pore size of nonwoven fabric made of fibres of different deniers: (a) - (c) — doffer speed *vs* cylinder speed at constant feeder speed of 0.19 m/min; (d) - (f) — doffer speed *vs* feeder speed at constant cylinder speed of 175 m/min; and (g) -(i) — cylinder speed *vs* feeder speed at constant doffer speed of 6 m/min

decrease and then an increase in the mean flow pore size because the initial decrease in mean flow pore size is highly influenced by the increase in cylinder and doffer speeds but later increase is influenced by the increase in feeder speed. The observed trends of 3 denier fibre are equally applicable to other denier fibres. The effect of fibre denier on the mean flow pore size is obvious due to the reasons as explained earlier.

Figures 4 (g) - (i) show the 3D surface plots of feeder speed *vs* cylinder speed at a constant doffer speed in relation to mean flow pore size of fabric made from different denier fibres. The mean flow pore size of 3 denier fabric shows a decrease and then an increase with the increase in cylinder speed, but increase in feeder speed depicts a slight decrease and then increase in mean flow pore size. Similar trends are also observed in fabrics made from 4 and 6 denier

fibres. The mean flow pore size follows a decrease and then increase with the increase in both feeder speed and cylinder speed at different doffer speeds. Increase in doffer speed also follows similar trends of mean flow pore size. The increase in feeder, cylinder and doffer speeds shows an initial decrease and then an increase in the value of mean flow pore size. Dominance of structural indices regulated by carding parameters explains the obtained trend of mean flow pore size.

3.3.1 Optimisation of Carding Parameters in Relation to Mean Flow Pore Size

The carding parameters are optimised for nonwoven fabrics made from fibres of different deniers to achieve the minimum mean flow pore size. The minimum mean flow pore size of fabric made of3denier is obtained at 0.14 m/min, 125.68 m/min and 4.51 m/min of feeder, cylinder, and doffer speeds respectively. The feeder, cylinder, and doffer speeds at 0.14 m/min, 114.21 m/min and 4.32 m/min respectively record the minimum pore size for the fabric made of fibre of 4 denier whereas the fabric made of 6 denier provides the minimum mean flow pore size at 0.15 m/min, 107.76 m/min and 4.20 m/min of feeder, cylinder, and doffer speeds respectively. The results depict corresponding minimum mean flow pore size at different combinations of carding parameters for fibre of different deniers.

3.3.2 Influence of Structural Indices on Mean Flow Pore Size

A regression model of nonlinear process is established between the mean flow pore size and the measured structural indices as shown in the following equations having R^2 values of 0.879, 0.804, 0.851 respectively:

3 denier fabric

$$\text{Mean flow pore size} = -356.044 - 1341.580 \times X_1 - 140.470 \times X_2 + 569.570 \times X_3 + 1825.060 \times X_1^2 + 165.632 \times X_2^2 - 123.002 \times X_3^2 \quad ...(20)$$

4 denier fabric

$$\text{Mean flow pore size} = -1215.240 - 2503.650 \times X_1 + 5063.580 \times X_2 + 18.130 \times X_3 + 5610.780 \times X_1^2 - 4273.110 \times X_2^2 - 3.555 \times X_3^2 \quad ... (21)$$

6 denier fabric

$$\text{Mean flow pore size} = 37.522 + 134.826 \times X_1 - 407.054 \times X_2 + 77.017 \times X_3 - 253.064 \times X_1^2 + 364.614 \times X_2^2 - 14.383 \times X_3^2 \quad \ldots(22)$$

The R^2 values indicate the dominance of structural indices in regulating the mean flow pore size of nonwoven fabrics made of fibre of different deniers. The mean flow pore size is highly influenced by coefficient of relative fibre parallelisation followed by proportion of curved fibre ends and anisotropy of inclination angle of the fibre.

3.4 Filtration Efficiency

The influence of carding parameters on the filtration efficiencies of fabrics made of different denier fibres for 10 µm particle size is summarised in Table 2. It is to be noted that the variance analysis is carried out for the filtration efficiency of nonwoven fabrics made from 3,4 and 6 denier fibres for 10 µm particles. Table 7 shows the variance analysis for nonwoven fabric made from 3 denier fibre.

The response surface equations for filtration efficiencies of nonwoven fabrics made from 3,4 and 6 denier fibres for 10 µm particles in terms of coded factors and significant model terms is represented in the following equations:

3 denier fabric

$$\text{Filtration efficiency} = 58.7026 - 3.1611 \times A + 4.6716 \times B + 1.5569 \times C - 0.1215 \times AB + 1.0427 \times AC - 0.0514 \times BC - 1.0717 \times A^2 - 4.8838 \times B^2 - 3.1860 \times C^2 \quad ...(23)$$

4 denier fabric

$$\text{Filtration efficiency} = 48.9278 - 2.8040 \times A + 4.3436 \times B + 0.7562 \times C - 0.1744 \times AB + 1.8183 \times AC + 0.0137 \times BC - 1.0615 \times A^2 - 3.9926 \times B^2 - 2.7920 \times C^2 \quad \ldots(24)$$

6 denier fabric

$$\text{Filtration efficiency} = 34.6041 - 1.8515 \times A + 2.3839 \times B + 1.1420 \times C - 0.0161 \times AB - 0.0160 \times AC - 0.0322 \times BC - 0.5489 \times A^2 - 0.7812 \times B^2 + 0.6310 \times C^2 \quad \ldots(25)$$

Table 7 — Variance analysis of filtration efficiency of 3 denier nonwoven fabric

Source	Sum of squares	df	Mean square	F-value	p-value	Significance
Model	396.66	9	44.07	33.24	0.0006	Significant
A-Feeder speed	79.94	1	79.94	60.29	0.0006	
B-Cylinder speed	174.59	1	174.59	131.68	< 0.0001	
C-Doffer speed	19.39	1	19.39	14.63	0.0123	
B^2	88.07	1	88.07	66.42	0.0005	
C^2	37.48	1	37.48	28.27	0.0031	
Residual	6.63	5	1.33			
Lack of fit	3.92	3	1.31	0.9624	0.5459	Not significant
Pure error	2.71	2	1.36			
Cor total	403.29	14				

These equations are used to draw the 3D surface plots of considered carding parameters in relation to filtration efficiencies for 10 µm particles of fabrics.

Figures 5 (a) - (c) show the 3D surface plots of cylinder speed *vs* doffer speed at different feeder speeds in relation to filtration efficiency for 10 µm size particles of nonwoven fabric made from 3, 4 and 6 denier fibres respectively. The results and 3D surface plots show an increase in filtration efficiency with increase in cylinder as well as doffer speeds. However, with further increase in speeds, a decrease in filtration efficiency is noticed at constant feeder speed. A decrease in filtration efficiency is observed with the increased feeder speed. The observed trends are valid for 10 µm size particles of fabrics made of 3 and 4 denier fibres. For fabrics made of 6 denier

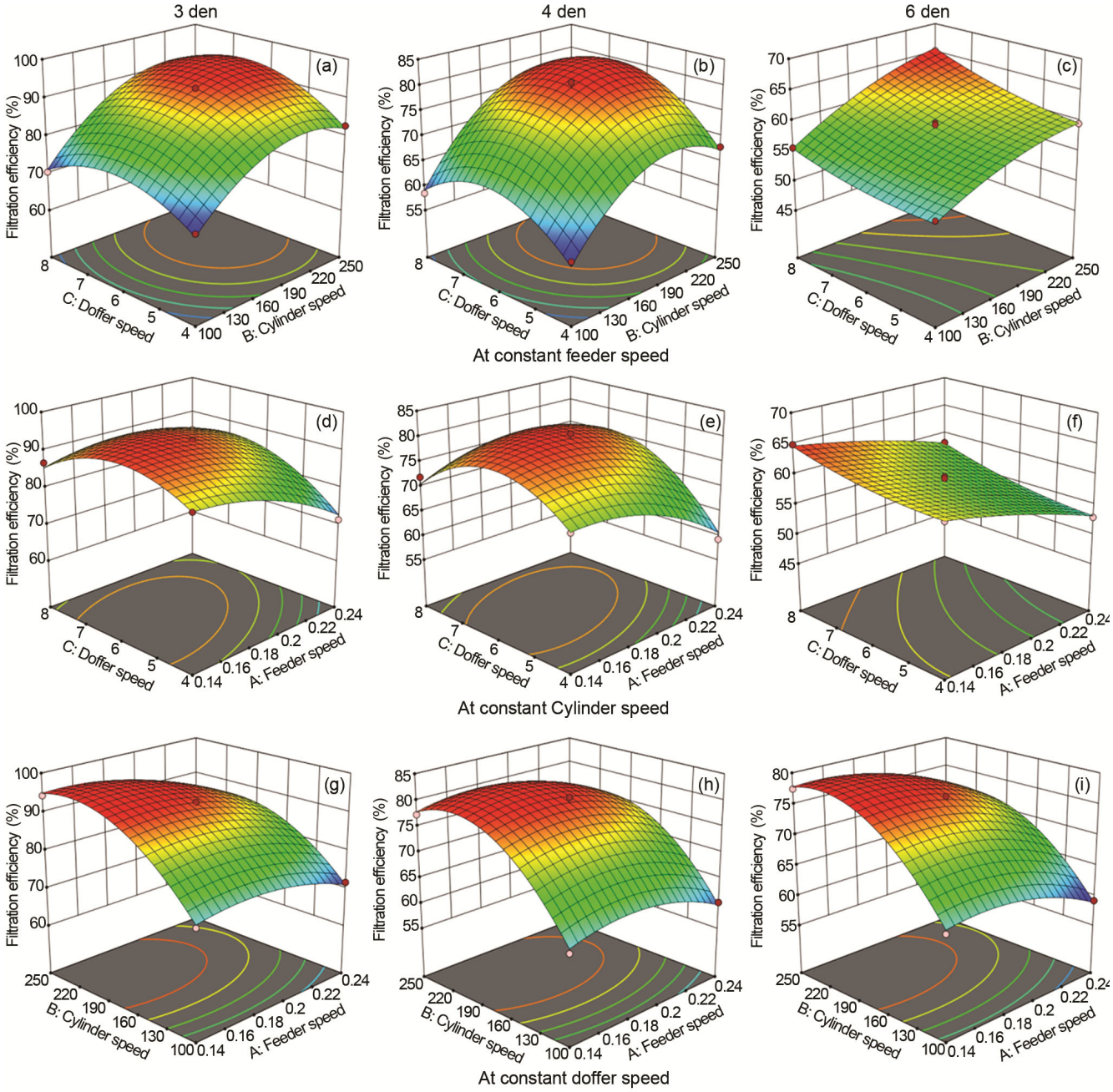

Fig. 5 — Filtration efficiency for 10 µm particle size of nonwoven fabric made of fibre of different deniers: (a) - (c) — doffer speed *vs* cylinder speed at constant feeder speed of 0.19 m/min; (d) - (f) — doffer speed *vs* feeder speed at constant cylinder speed of 175 m/min; and (g) - (i) — cylinder speed *vs* feeder speed at constant doffer speed of 6 m/min

fibres, an increase in filtration efficiency with the increase of both cylinder and doffer speeds at different feeder speeds is observed. An increase in filtration efficiency with an increase in feeder speed is also noticed.

Filtration efficiency depends on fibre orientation, fabric thickness, mean flow pore size, pressure drop, etc. The fibre orientation in the carded web is influenced by the carding parameters, such as proportion of curved fibre ends, coefficient of relative fibre parallelization and anisotropy of inclination angle of fibre, and this is responsible for obtained trends of filter efficiency. As described above, fabric thickness and mean flow pore size also support the trends of filtration efficiency. The simultaneous increase of all carding parameters shows an increase and then a decrease in the filtration efficiency. The filtration efficiency also decreases with the increase in fibre denier. It is important to highlight that filtration efficiency depends on fibre deniers, but fibre orientation influenced by fibre deniers also plays an equally important role in deciding the filtration efficiency. Moreover, random distribution of a higher number of smaller size pores in case of finer fibres, as compared to coarser fibres, enhances the filtration efficiency.

Figures 5 (d) - (f) show the 3D surface plots of feeder speed *vs* doffer speed at different cylinder speeds in relation to filtration efficiency for 10 µm size particles of nonwoven fabrics made from 3,4 and 6 denier fibres respectively. The 3D surface plots for fabrics made from 3 denier fibres reveal an increase and then a decrease in filtration efficiency with the increase in feeder speed as well as doffer speed at a constant cylinder speed. However, filtration efficiency exhibits an increase and then a slight decrease with the increase in cylinder speed. The disorientation of fibres caused by the increase in feeder speed gets compensated by cylinder speed and doffer speed. However, any further increase in feeder speed hampers the fibre orientation. The obtained trends are also followed by nonwoven fabrics made of 4 and 6 denier fibres. With the increase in feeder, cylinder, and doffer speeds, the filtration efficiency increases. However, a slight decrease is noticed with higher cylinder speed. This is because the increase in cylinder speed reduces the proportion of curved fibre ends but increases the coefficient of relative fibre parallelisation along with anisotropy of inclination angle of fibre.

Figures 5 (g) - (i) show the 3D surface plots of feeder speed *vs* cylinder speed at different doffer speeds in relation to filtration efficiency for 10 µm size particles of nonwoven fabric made from 3, 4 and 6 denier fibres respectively. The results of filtration efficiency of nonwoven fabrics made of 3 denier fibres show an increase and then a decrease with the increase in feeder speed as well as cylinder speed at a constant doffer speed. The increase in doffer speed also shows the same trends of filtration efficiency. The same trends are also observed for nonwoven fabrics made from 4 and 6 denier fibres. Initial increase in feeder and cylinder speeds at a constant doffer speed exerts positive influence on fibre orientation. However, further increase in feeder and cylinder speeds at a constant doffer speed increases proportion of curved fibre ends, but decreases coefficient of relative fibre parallelisation and anisotropy of inclination angle of fibre. This causes a reduction in the filtration efficiency. However, on further increasing the doffer speed, negative effect of structural indices results in lower filtration efficiency. It is seen that the filtration efficiency increases and then decreases with the increase in feeder, cylinder, and doffer speeds.

3.4.1 Optimisation of Carding Parameters in Relation to Filtration Efficiency

The carding parameters are optimised for nonwoven fabrics made of fibres of different deniers in order to obtain maximum filtration efficiency. The fabric made of 3 denier fibres depicts maximum efficiency at 0.14 m/min, 101.59 m/min and 4.06 m/min of feeder, cylinder, and doffer speeds respectively. However, 0.14 m/min, 120.55 m/min and 5.01 m/min of feeder, cylinder, and doffer speeds respectively are achieved for maximum efficiency of fabric made of 4 denier fibres. Fabric made of 6 denier fibre registers maximum filter efficiency at 0.17 m/min, 131.06 m/min and 5.72 m/min of feeder, cylinder, and doffer speeds respectively. To obtain maximum filtration efficiency, nonwoven fabrics made of fibre of different deniers need to be processed at different combinations of carding parameters.

3.4.2 Influence of Structural Indices on Filtration Efficiency

A regression model of nonlinear process is established between the filtration efficiency for 10 µm particles of nonwoven fabrics made of fibres of different deniers and structural indices as shown in

the following equations having R^2 value as 0.971, 0.937, 0.976respectively:

3 denier fabric

$$\text{Filtration efficiency} = 0.4141 + 1.9345 \times X_1 + 159.2780 \times X_2 + 0.1948 \times X_3 + 2.6951 \times X_1^2 + 2.7375 \times X_2^2 + 0.0299 \times X_3^2 \quad \ldots(26)$$

4 denier fabric

$$\text{Filtration efficiency} = -169.6650 - 490.8760 \times X_1 + 1286.1600 \times X_2 - 72.1369 \times X_3 + 1064.1700 \times X_1^2 - 984.7540 \times X_2^2 + 11.5177 \times X_3^2 \quad \ldots(27)$$

6 denier fabric

$$\text{Filtration efficiency} = -48.0443 - 451.3440 \times X_1 - 124.8320 \times X_2 + 103.0430 \times X_3 + 971.7800 \times X_1^2 + 160.2630 \times X_2^2 - 15.1314 \times X_3^2 \quad \ldots(28)$$

The obtained R^2 values indicate a strong correlation between filtration efficiency for 10 µm particle sizes and structural indices. The coefficient of relative fibre parallelisation regulates the filtration efficiency the most followed by proportion of curved fibre ends and anisotropy of inclination angle of fibre for 3 and 4 denier nonwoven fabrics. For 6 denier fabric, the proportion of curved fibre ends plays a significant role followed by coefficient of relative fibre parallelisation and anisotropy of inclination angle of fibre. As explained earlier, the use of nonwoven structures having better-oriented fibres leads to an increase in number of smaller pore sizes, which helps in the effective trapping of dust particles, thus enhancing the filtration efficiency of the nonwoven fabric.

3.5 Pressure Drop

The effect of carding parameters on the pressure drop of fibres of different deniers is represented in Table 2. The variance analysis of pressure drop for nonwoven fabrics made from 3, 4 and 6 denier fibres has been carried out. The variance analysis results of pressure drop for nonwoven fabrics made of 3 denier fibres are shown in Table 8.

The response surface equations for pressure drop in terms of coded factors and significant model terms for 3, 4 and 6 denier fibres are represented by the following equations:

3 denier fabric

$$\text{Pressure drop} = 108.4470 - 4.3675 \times A + 8.3962 \times B + 4.2912 \times C + 0.4600 \times AB + 2.3600 \times AC + 2.1125 \times BC - 3.4371 \times A^2 - 8.1746 \times B^2 - 6.8596 \times C^2 \quad \ldots(29)$$

4 denier fabric

$$\text{Pressure drop} = 96.8533 - 3.6262 \times A + 8.8262 \times B + 2.5575 \times C - 1.18 \times AB + 4.3575 \times AC + 1.5525 \times BC - 3.6117 \times A^2 - 8.4367 \times B^2 - 7.3792 \times C^2 \quad \ldots(30)$$

Table 8 — Variance analysis of pressure drop for 3 denier nonwoven fabric

Source	Sum of squares	df	Mean square	F-value	p-value	Significance
Model	1316.65	9	146.29	80.37	< 0.0001	Significant
A-Feeder speed	152.60	1	152.60	83.83	0.0003	
B-Cylinder speed	563.98	1	563.98	309.83	< 0.0001	
C-Doffer speed	147.32	1	147.32	80.93	0.0003	
AC	22.28	1	22.28	12.24	0.0173	
BC	17.85	1	17.85	9.81	0.0259	
A^2	43.62	1	43.62	23.96	0.0045	
B^2	246.73	1	246.73	135.55	< 0.0001	
C^2	173.74	1	173.74	95.44	0.0002	
Residual	9.10	5	1.82			
Lack of fit	8.37	3	2.79	7.64	0.1180	Not significant
Pure error	0.7309	2	0.3654			
Cor total	1325.75	14				

6 denier fabric

$$\text{Pressure drop} = 80.6200 - 3.7375 \times A + 6.8587 \times B + 2.3362 \times C - 1.5300 \times AB + 3.5100 \times AC + 2.0225 \times BC - 3.5062 \times A^2 - 6.8138 \times B^2 - 6.6437 \times C^2 \quad \ldots(31)$$

The R^2 values 0.974, 0.917 and 0.949 represent the correlation between pressure drop and carding parameters. These equations are used to draw the 3D surface plots of considered carding parameters in relation to the pressure drop of fabrics.

Figures 6 (a) - (c) show the 3D surface plots of cylinder speed *vs* doffer speed at different feeder speeds in relation to pressure drop of nonwoven fabric made from 3,4 and 6 denier fibres respectively. The data obtained from the equations and corresponding 3D surface plots reveal an increase and then a decrease in pressure drop of fabrics made of 3 denier fibres with the increase in the cylinder as well as doffer speeds at constant feeder speed. With the increase in feeder speed, the pressure drop is found to decrease. The nonwoven fabrics made of 4 and 6 denier fibres also show similar trends. It is known that the increase in cylinder and doffer speeds increases the coefficient of relative fibre parallelisation and anisotropy of inclination angle of fibre, but it reduces the proportion of curved fibre ends. The measured structural indices are positively influenced by fibre straightening and parallelization in the carded web. Hence, this leads to close packing of the fibres such that the space between the fibres is reduced, thereby causing lesser fabric thickness and smaller pores contribute to build up pressure across the fabric. However, fibres get disoriented towards higher

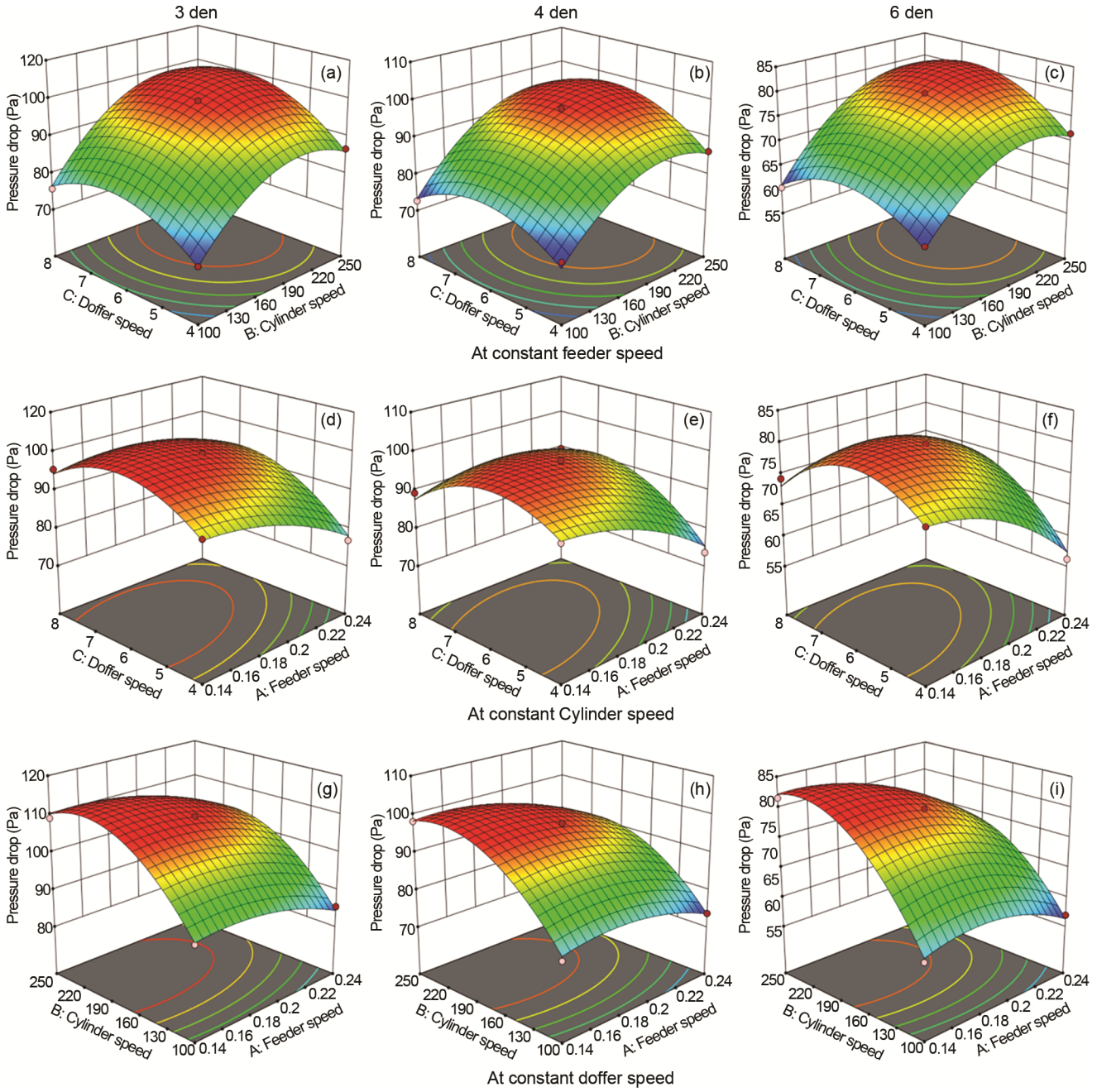

Fig. 6 — Pressure drop of nonwoven fabric made of fibre of different deniers: (a) - (c) — doffer speed *vs* cylinder speed at constant feeder speed of 0.19 m/min; (d) - (f) — doffer speed *vs* feeder speed at constant cylinder speed of 175 m/min; and (g) -(i) —cylinder speed *vs* feeder speed at constant doffer speed of 6 m/min

cylinder and doffer speeds, which causes reduction in the pressure drop values. The increase in feeder speed shows a decrease in pressure drop. The increase in feeder speed imparts a negative influence on structural indices which results in more space between the fibres due to disorientation of fibres, accordingly, a reduction in pressure drop is noticed. Subsequently, high fabric thickness and mean flow pore size also support the reduction in pressure drop. Simultaneous increase in feeder, cylinder, and doffer speeds shows the same trend.

It is observed that an increase in fibre denier reduces the pressure drop. With an increase in fibre denier, the proportion of curve fibre ends reduces and the coefficient of relative fibre parallelisation increases. Therefore, domination of fibre diameter

over improved orientation of fibres with the increase in fibre deniers governs the pressure drop. Thus, when the dust-laden air passes through the nonwoven fabric made of fibres of coarser denier, the particles do not get trapped easily. Accordingly, the process prolongs the successive deposition of dust on the layer and offers less resistance to air flow, resulting in lower pressure drop.

Figures 6 (d) - (f) show the 3D surface plots of feeder speed *vs* doffer speed at different cylinder speeds in relation to pressure drop of nonwoven fabric made from 3,4 and 6 denier fibres respectively. The fabrics made from 3 denier fibres show an increase and then a decrease in pressure drop with increase in feeder speed as well as doffer speed at constant cylinder speed. The same pattern of pressure drop is also observed by the other two fibre deniers. The increase in cylinder speed positively influences the structural indices, which leads to a reduction in pressure drop due to better consolidation of the fibres. The disorientation caused by feeder speed is taken care of by cylinder and doffer speeds. However, further increase in feeder speed increases the proportion of curved fibre ends and decreases the coefficient of relative fibre parallelisation and anisotropy of inclination angle of fibre. Moreover, an increase in doffer speed leads to further deterioration of the structural indices, which results in an increase in pressure drop across the nonwoven fabric. However, at higher cylinder speeds, fibres get disoriented leading to lower pressure drop values. Pressure drop shows an increase and then decrease with a simultaneous increase in feeder, cylinder, and doffer speeds. The results of mean flow pore size, as discussed above, support the trend of pressure drop. The pressure drop is found to decrease with the increase in fibre denier.

Figures 6 (g) - (i) show the 3D surface plots of feeder speed *vs* cylinder speed at different doffer speeds in relation to pressure drop of nonwoven fabric made from 3, 4and 6 denier fibres respectively. The pressure drop of fabrics made of 3 denier fibres shows an increase and then a decrease with the increase in feeder speed as well as cylinder speeds at a constant doffer speed. The same pattern of pressure drop is also observed by 4 and 6 denier fibres. This decrease in pressure drop is due to better fibre orientation influenced by feeder and cylinder speeds. However, as the feeder speed increases, the structural indices exert a negative influence on the fibre orientation, thus reducing the pressure drop. It is observed that with an increase in doffer speed, pressure drop increases followed by a subsequent decrease. The pressure drop is found to increase and then decrease with a simultaneous increase in feeder, cylinder, and doffer speeds.

3.5.1 Optimisation of Carding Parameters in Relation to Pressure Drop

The carding parameters are optimised for nonwoven fabric made of fibres of different deniers, keeping the pressure drop to a minimum. It is observed that the feeder, cylinder, and doffer speeds for fabrics made of 3 denier fibres depict minimum pressure drop at 0.15 m/min, 249.19 m/min and 7.82 m/min respectively, but 4 denier fibres achieve minimum value at 0.14 m/min, 247.36 m/min and 7.61 m/min of feeder, cylinder, and doffer speeds respectively. Fabrics made of 6 denier fibres provide minimum value at 0.14 m/min, 244.17 m/min and 8.0 m/min of feeder, cylinder, and doffer speeds respectively. It is noticed again that nonwoven fabrics made of fibres of different deniers reveal different combinations of carding parameters with respect to pressure drop.

3.5.2 Influence of Structural Indices on Pressure Drop

A regression model of nonlinear process is established between the pressure drop of fabric made of fibre of different deniers and the structural indices as shown in the following equations with R^2 values as 0.942, 0.934, 0.922 respectively:

3 denier fabric

$$\text{Pressure drop} = -113.936 - 485.110 \times X_1 + 759.557 \times X_2 + 51.070 \times X_3 + 709.007 \times X_1^2 - 603.991 \times X_2^2 - 10.271 \times X_3^2 \quad ...(32)$$

4 denier fabric

$$\text{Pressure drop} = -21.4793 + 87.4334 \times X_1 + 124.6270 \times X_2 + 12.2547 \times X_3 - 146.2610 \times X_1^2 + 5.0173 \times X_2^2 - 1.1362 \times X_3^2 \quad \ldots(33)$$

6 denier fabric

$$\text{Pressure drop} = 619.189 + 431.102 \times X_1 - 11175.400 \times X_2 + 1714.750 \times X_3 - 1414.440 \times X_1^2 + 8631.930 \times X_2^2 - 241.645 \times X_3^2 \quad ...(34)$$

The obtained R^2 values indicate that the pressure drop is greatly influenced by measured structural indices. The coefficient of relative fibre parallelisation plays a vital role in regulating the pressure drop followed by proportion of curved fibre ends and

Table 9 — Optimised carding parameters and denier specific fabric properties

Fibre denier	Feeder speed m/min	Cylinder speed m/min	Doffer speed m/min	Thickness mm	Bursting strength, bar	Mean flow pore size µm	Filtration efficiency %	Pressure drop Pa	Desirability
3	0.140	245.36	4.01	2.33	16.02	25.02	86.04	100.56	0.698
4	0.220	165.78	5.59	2.89	14.60	26.12	74.42	92.77	0.693
6	0.220	148.23	6.27	3.38	12.90	36.34	62.08	69.27	0.767

Table 10 — Predicted and experimental values of properties at optimised carding parameters

Fibre denier	Feeder speed m/min	Cylinder speed m/min	Doffer speed m/min	Thickness mm		Bursting strength bar		Mean flow pore size, µm		Filtration efficiency, %		Pressure drop Pa	
				Pred.	Exp.	Pred.	Exp.	Pred.	Exp.	Pred.	Exp.	Pred.	Exp.
3	0.140	245.36	4.01	2.33	2. 29	16.02	15.72	25.02	23.98	86.04	87.42	100.56	102.37
4	0.220	165.78	5.59	2.89	2.94	14.60	13.85	26.12	27.42	74.42	73.03	92.77	90.54
6	0.220	148.23	6.27	3.38	3.32	12.90	12.24	36.34	33.67	62.08	65.07	69.27	71.01

Pred.- Predicted. Exp.- Experimental.

anisotropy of inclination angle of fibre for 3 denier nonwoven fabric, while for 4 and 6 denier nonwoven fabrics, it is coefficient of relative fibre parallelisation followed by anisotropy of inclination angle of fibre and proportion of curved fibre ends. The increase in coefficient of relative fibre parallelisation and reduction in the value of proportion curved fibre ends result in the better orientation of the fibres. Improved orientation of fibres provide more closeness among the fibres and offers higher pressure drop.

3.6 Optimisation of Carding Parameters for Desired Properties of Nonwoven Fabrics

The overall optimisation of carding parameters for specific fibre denier is carried out to design desired filter media, using Design Expert software's desirability function. The desirability function is associated with the target responses, where 0 is assigned to the undesired response, while the acceptable response values lie between 0 and 1. The desirability function, therefore, aids in identifying the most advantageous and acceptable location in the design space that satisfies the set goals for responses. The target is set to obtain maximum filtration efficiency at minimum pressure drop with minimum pore size along and moderate value of bursting strength for all considered fibre deniers. Accordingly, the importance of properties is prioritised depending upon their applicability. The optimised carding parameters with predicted fabric properties for respective deniers of fibre are given in Table 9. The results depict that nonwoven fabrics made of fibres of different deniers provide different targeted properties at an exclusive combination of carding parameters. Thus, it becomes imperative to state that the respective fibre denier needs a specific and distinct combination of carding parameters to provide desired properties.

Taking a step further, the optimised carding parameters are re-validated by preparing the nonwoven fabrics using the optimised carding parameters for respective fibre deniers. Table 10 shows both the predicted and experimental values of fabric properties.

Table 10 reveals that experimental values of fabric properties are quite close to the predicted values without much significant difference. This exercise confirms the reproducibility of fabric properties by using optimised carding parameters.

4 Conclusion

This study represents an elaborate analysis of the properties of nonwoven fabrics made from fibres of different deniers at different combinations of carding parameters. The properties of nonwoven fabrics are critically analysed to discover that the nonwoven structures, developed by considering different sets of carding parameters, also possess different physical and functional properties. The need to optimise the carding parameters specific to fibre deniers resulted in an improvement of the filtration performance of the nonwoven fabrics having lower values of thickness, mean flow pore size and pressure, besides acquiring higher filtration efficiency. The relationship between structural indices and nonwoven properties provides insight into the inevitable importance of structure in designing a filter media. Hence, this work highlights the technique to modulate the structure of the nonwoven filter fabrics by regulating both the fibre denier as well as carding parameters for desired properties.

References

1 Lamb G E R, Miller B & Constanza P, *Text Res J*, 45 (1975) 452.

2 Das D, Das S & Ishtiaque S M, *Fibers Polym*, 15 (2014) 1456.

3 Pradhan A K, Das D & Chattopadhyay R, *J Ind Text*, 45 (2016) 1308.

4 Payen J, Vroman P, Lewandowski M & Perwuelz A, *Text Res J*, 82 (19) (2012) 1948.

5 Thilagavathi G, Muthukumar N, Neelakrishnan S & Egappan R, *J Ind Text*, 48 (10) (2019) 1566.

6 Thangadurai K, Thilagavathi G & Bhattacharyya A, *J Text Inst*, 105 (12) (2014) 1319.

7 Anandjiwala R D & Boguslavsky L, *Text Res J*, 78 (7) (2008)614.

8 Yousfani S H S, Gong R H & Porat I, *Polym Compos*, 24 (1) (2016) 65.

9 Li W, Shen S & Li H, *Adv Powder Technol*, 27 (2) (2016) 638.

10 Kothari V K, Das A & Sarkar A, *Indian J Fibre Text Res*, 32 (2) (2007) 196.

11 Ventura H, Ardanuy M, Capdevila X, Cano F & TorneroJ, *J Text Inst*, 105 (10) (2014) 1065.

12 Dixit P, Ishtiaque S M & Roy R, *Compos B Eng*, 182 (2020) 107654.

13 Neckar B & Das D, *J Text Inst*, 103 (3) (2012) 330.

14 Roy R & Ishtiaque S M, *Indian J Fibre Text Res*, 44 (3) (2019) 321.

15 Saghafi R, Zarrebini M & Moezzi M, *J Text Polym*, 5 (1) (2017) 218.

16 Roy R & Ishtiaque SM, *Indian J Fibre Text Res*, 44 (2) (2019) 131.

17 Roy R, Ishtiaque SM & Dixit P, *J Text Inst*, 51 (2020) 4801S. doi:10.1177/1528083720910706.

18 Dixit P & Ishtiaque SM, *J Text Inst*, 114 (2022) 622. doi: 10.1080/00405000.2022.2059905

19 Lindsley CH, *Text Res J*, 21 (1951) 39.

20 Neckar B & Das D, *J Text Inst*, 103 (2012) 330.